

# Scaling of Taylor flow in small square channels of different size

Wörner, Martin

Karlsruhe Institute of Technology (KIT), Institute for Nuclear and Energy Technologies (IKET)  
P.O. Box 3640, 76021 Karlsruhe, Germany  
E-mail: martin.woerner@kit.edu

## Abstract

We study the influence of channel size on co-current downward Taylor flow in a square channel by a volume-of-fluid method. Simulations for three different hydraulic diameters ( $D_h = 0.5, 1, 2$  mm) show that the non-dimensional bubble velocity, bubble diameter and specific interfacial area scale with the capillary number while the influence of the Reynolds and Eötvös number is negligible for the range of parameters investigated.

**Keywords:** Taylor flow, micro process engineering, direct numerical simulation, monolith reactors

## 1. Introduction

In small channels, slug flow often occurs in the form of Taylor flow. In this flow pattern elongated bullet-shaped gas bubbles that almost fill the channel cross-section (Taylor bubbles) are separated by liquid slugs which are free from gas entrainment. Taylor flow is attractive for multiphase micro process engineering because the high interfacial area per unit volume and the thin liquid film allow for very efficient gas/liquid and gas/liquid/solid heat and mass transfer.

An actual field of research in chemical process engineering is the utilization of the potential advantages of Taylor flow in multiphase reactors such as monolith reactors with catalytic walls, e.g. for Fischer-Tropsch synthesis (Guettel *et al.*, 2008; Liu *et al.*, 2009). Monolith reactors consist of a monolithic block (often made from ceramics) with a large number of straight parallel channels. Often, the channel cross-section is rectangular or square with rounded corners due to the coating with a catalytically active washcoat. The hydraulic diameter  $D_h$  of the channels is typically in the range 0.5 – 5 mm (Boger *et al.*, 2004). Important hydrodynamic parameters of Taylor flow such as the liquid film thickness depend mainly on the capillary number  $Ca = \mu_L U_B / \sigma$  (Taylor, 1961; Bretherton, 1961; Kreuzer *et al.*, 2005), where  $\mu_L$  is the liquid dynamic viscosity,  $\sigma$  is the coefficient of surface tension and  $U_B$  is the bubble velocity. In contrast to  $Ca$ , the Reynolds number  $Re = \rho_L D_h U_B / \mu_L$  and the Eötvös number  $Eö = g (\rho_L - \rho_G) D_h^2 / \sigma$  both involve a length scale (which is here the channel hydraulic diameter  $D_h$ ). Changing  $D_h$  (i.e. the channel size) while keeping  $Ca$  constant is thus associated with a change of  $Re$  and  $Eö$  (and

therefore a change of the relative importance of inertial and buoyant forces as compared to viscous and interfacial forces).

In this paper, we study numerically the influence of the channel size on co-current downward Taylor flow in a square channel by a volume-of-fluid method with piecewise linear interface calculation (PLIC). We perform numerical simulations for three different hydraulic diameters ( $D_h = 0.5$  mm, 1 mm, 2 mm) and investigate in how far hydrodynamic parameters of Taylor flow scale with  $Ca$ , or additionally depend on  $Re$  and  $Eö$ , respectively.

## 2. Numerical simulation of Taylor flow

### 2.1 Numerical method

In this section we give a short description of the numerical method and the computational set-up. The time-dependent three-dimensional computations are performed with an in-house computer code, called TURBIT-VOF. This code solves the Navier-Stokes equation with surface tension term in non-dimensional single field formulation for two incompressible Newtonian fluids with constant viscosity and coefficient of surface tension on a regular staggered Cartesian grid by a finite volume method. All spatial derivatives are approximated by central differences. Time integration is performed by an explicit third order Runge-Kutta method. A divergence free velocity field at the end of each time step is enforced by a projection method, in which the resulting Poisson equation is solved by a conjugate gradient technique. The dynamic evolution of the interface is computed by an un-split volume-of-fluid method with piecewise planar interface reconstruction. For further details about the governing equations and the numerical method we refer to Öztaskin *et al.* (2009).

## 2.2 Computational set-up

For the computational set-up, we follow the procedure of our previous papers and consider one unit cell, which consists of one gas bubble and one liquid slug. We use in axial (vertical) direction periodic boundary conditions to mimic the influence of the trailing and leading bubble in Taylor flow. No-slip boundary conditions are applied at the four lateral walls of the square channel.

In this paper we consider three square channels with different cross-section, namely 0.5 mm × 0.5 mm, 1 mm × 1 mm and 2 mm × 2 mm. In the code, the different dimensions are realized by setting the reference length scale  $L_{ref}$  (which is equal to  $D_h$ ) to 0.5 mm, 1 mm and 2 mm, respectively, while the reference velocity is always  $U_{ref} = 0.12$  m/s. For all cases the non-dimensional axial length of the unit cell is  $L_{uc} / L_{ref} = 4$ . This computational domain is discretized by a regular Cartesian grid with 80×320×80 mesh cells.

In accordance to the experiments by Bauer (2007) (see also Keskin *et al.*, 2010) we use as continuous liquid phase squalane ( $C_{30}H_{62}$ ) while the disperse gas phase is nitrogen. These experiments were performed at a pressure of 20 bar. The corresponding fluid properties of nitrogen used in the simulations are  $\rho_G = 23.6$  kg/m<sup>3</sup> and  $\mu_G = 0.01804$  mPa s. Since the physical properties of squalane at a pressure of 20 bar are not available to our knowledge, we use the known (constant) properties at standard conditions which are  $\rho_L = 802$  kg/m<sup>3</sup>,  $\mu_L = 0.029$  Pa s, and  $\sigma = 0.0286$  N/m. The Eötvös number for the three channels is then 0.0667, 0.267 and 1.068, respectively.

To save CPU time, the simulations are not started from fluid at rest but from case 4\_40\_A or 4\_40\_B in Keskin *et al.* (2010), where  $D_h = 1$  mm. In all simulations the gas hold in the unit cell is  $\varepsilon = 0.4$ . Starting from these initial conditions, the flow is driven by a prescribed source term in the axial momentum equation,  $II_y$ , which corresponds to the net driving force due to gravity and pressure drop along the unit cell  $\Delta p_{uc}$ , so that  $II_y = Eu_{ref} L_{ref} / L_{uc} - Fr_{ref}$ . Here,  $Eu_{ref} = \Delta p_{uc} / (\rho_L U_{ref}^2)$  and  $Fr_{ref} = g L_{ref} / U_{ref}^2$  are the reference Euler and Froude number, respectively. In the course of the simulations, the evolution from the initial velocity field and bubble shape toward a fully developed Taylor flow is computed. This requires typically a few 10,000 up to 100,000 time steps. Here, a non-dimensional time step width  $\Delta t = 4E-5$  is used. In Table 1 we give a list of all cases considered in the present study.

In the past we assumed that fully developed Taylor flow is achieved when the mean axial gas and liquid velocities in the computational domain are constant in time (and so are  $Ca$  and  $Re$ ). However, recently we observed that even then the bubble length and diameter may slight change in time. In this sense, some cases listed in Table 1 are not finished and are further advanced in time. The same holds for some cases in Keskin *et al.* (2010).

**Table 1** Overview on simulations of co-current downward Taylor flow in a square channel.

$D_h$ [mm]	$II_y$ [-]	$U_B$ [m/s]	$J$ [m/s]	$Ca$ [-]	$Re$ [-]
0.5	-6	0.113	0.075	0.114	1.56
0.5	-7	0.145	0.094	0.151	2.06
0.5	-8	0.203	0.121	0.206	2.81
0.5	-9	0.260	0.149	0.264	3.60
0.5	-10	0.324	0.178	0.328	4.47
0.5	-11	0.410	0.217	0.416	5.67
0.5	-12	0.492	0.254	0.499	6.81
1	-5	0.251	0.147	0.255	6.95
1	-6	0.379	0.207	0.385	10.49
2	-2.9	0.185	0.117	0.188	10.24
2	-3.1	0.210	0.130	0.213	11.60
2	-3.3	0.239	0.146	0.243	13.23

## 3. Results and Discussion

### 3.1 Bubble shape

In Fig. 1 we show the computed steady bubble shape for the case with  $D_h = 2$  mm and  $II_y = -3.1$ . Also shown in Fig. 1 is the velocity field in two horizontal cross-sections. It is evident that the velocity field in the middle of the liquid slug is close to parabolic. We remark, that in all present simulations the capillary number is larger than 0.04 (see Table 1) so that the bubble is always axisymmetric. The visualizations of the bubble shape for the cases with  $D_h = 0.5$  mm show that with increase of  $Ca$  the curvature of the bubble front increases, while that of the bubble rear decreases (cf. Wörner, 2010).

### 3.2 Bubble velocity

In practical applications the flow rates of the phases are often prescribed so that the phase superficial velocities  $J_L$  and  $J_G$  and the total superficial velocity  $J = J_G + J_L$  are given. Of interest is the resulting bubble velocity which determines  $Ca$ . A common model to estimate  $U_B$  from a given value of  $J$  is the drift flux model (Zuber & Findlay, 1965)

$$U_B = C_0 J + U_{G,J} \quad (1)$$

Here,  $C_0$  is the distribution parameter and  $U_{G,J}$  is the drift velocity.

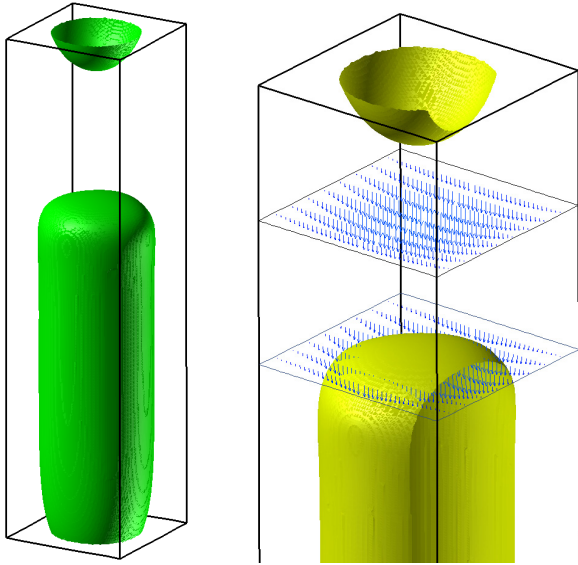


**Fig. 1** Computed steady bubble shape (left) and detail of the velocity field in the liquid slug and close to the bubble rear (right) for case  $D_h = 2$  mm with  $I_y = -3.1$ . Note that in the two horizontal directions only every 2<sup>nd</sup> respectively 8<sup>th</sup> vector is displayed and only a part of the bubble is shown.

In Fig. 2 we display  $U_B$  over  $J$ . As can be seen, the data for the different channels almost collapse to one curve and no notable influence of the channel size can be identified. However, the relation between  $U_B$  and  $J$  is only piecewise linear so that different values of  $C_0$  and  $U_{G-J}$  are required to fit the data by drift flux model for low and small values of  $J$ . The solid and dashed line in Fig. 2 represent the drift flux model with the values of  $C_0$  and  $U_{G-J}$  as obtained by Keskin *et al.* (2010) from numerical simulations of co-current downward Taylor flow in a square channel with  $D_h = 1$  mm for  $J < 0.109$  m/s and  $J > 0.109$  m/s, respectively. In Keskin *et al.* (2010) simulations were not only performed for  $L_{uc} / D_h = 4$  and  $\varepsilon = 0.4$  (as in the present study) but also for  $L_{uc} / D_h = 6$  and  $\varepsilon = 0.2$ . Fig. 2 shows that the present numerical results can well be described by the drift flux model with these parameters.

In Fig. 3 we display the ratio  $U_B / J$  as function of the capillary number. In this semi-logarithmic plot a very small influence of the channel size can be identified. It appears that for the same value of  $Ca$  the ratio  $U_B / J$  is slightly decreasing with increase of  $D_h$ . Also shown in Fig. 3 are experimental data of Thulasidas *et al.* (1995) for co-current upward Taylor flow of air bubbles in water in a 2 mm square channel and a correlation proposed by Liu *et al.* (2005) which reads (see also Keskin *et al.*, 2010)

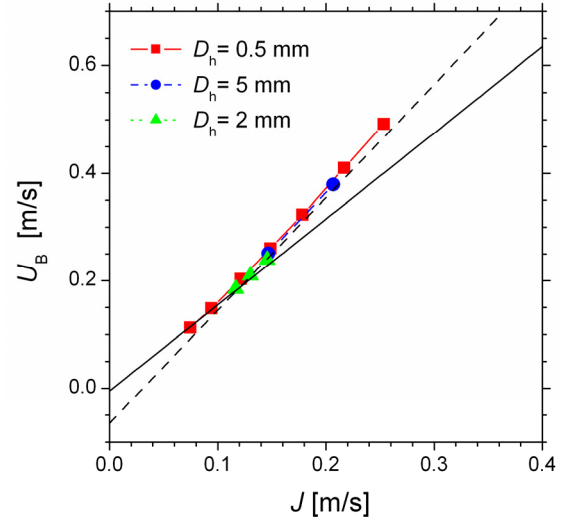


**Fig. 2** Bubble velocity versus total superficial velocity. The solid and dashed lines correspond to ( $C_0 = 1.6$ ,  $U_{G-J} = -0.005$  m/s) and ( $C_0 = 2.15$ ,  $U_{G-J} = -0.065$  m/s) respectively, see Keskin *et al.* (2010).

$$Ca \approx 4.47 \frac{(U_B / J - 1)^3}{(U_B / J)^2} \quad (2)$$

This correlation is obtained by fitting experimental results in capillaries with circular and square cross-section with  $D_h$  in the range of 0.9 – 3 mm using air and three different liquids. It can be seen that the present numerical data for downward flow are between those of the two latter references. However, they agree better with the data of Thulasidas *et al.* (1995).

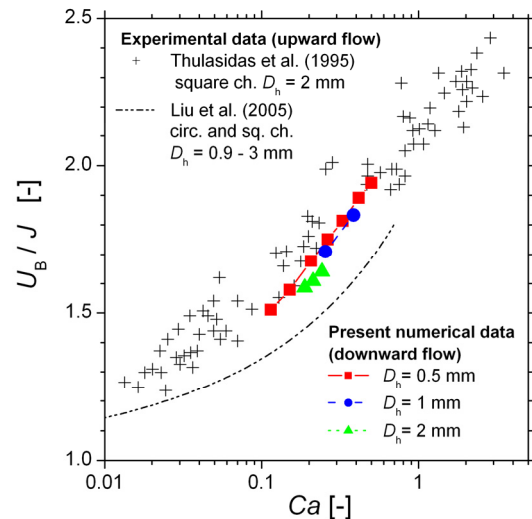


**Fig. 3** Ratio  $U_B / J$  as function of the capillary number. Comparison of present numerical results with experimental data from literature.

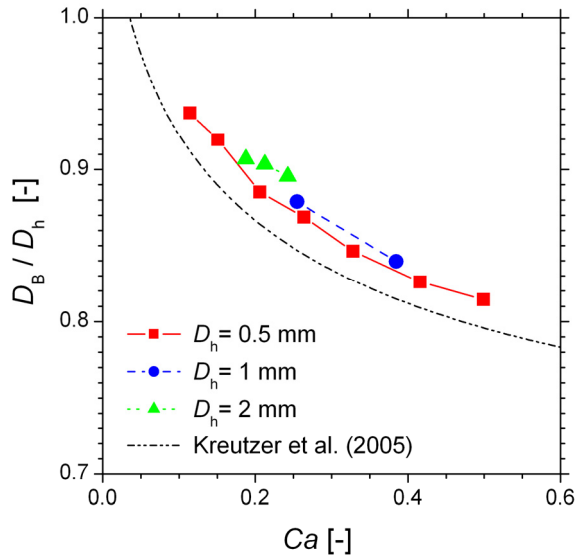


**Fig. 4** Non-dimensional bubble diameter versus capillary number.

### 3.3 Bubble diameter

An important parameter of Taylor flow in technical applications is the thickness of the liquid film which surrounds the bubble and separates it from the solid wall. The thinner the liquid film, the smaller is the resistance to mass transfer from the gas bubble to the catalytic washcoat. In a square channel, the thickness of the liquid film varies along the circumference of the bubble. In the present simulations, the bubble is axisymmetric, so that the bubble dimension and the liquid film thickness can be characterized in terms of the maximum diameter of the bubble,  $D_B$ .

In Fig. 4 we display the non-dimensional bubble diameter  $D_B / D_h$  as function of  $Ca$ . Again the influence of channel size is very small, though it appears that a larger channel size results in slightly higher values of  $D_B / D_h$ . Also shown in Fig. 4 is the correlation

$$\frac{D_{B,diag}}{D_h} = 0.7 + 0.5 \exp(-2.25Ca^{0.445}) \quad (3)$$

proposed by Kreutzer et al. (2005) for the bubble diameter in the diagonal direction of a square channel. In all present simulations the ratio  $D_B / D_h$  is larger than predicted by Eq. (3). We note that the data for  $D_h = 0.5$  mm in Fig. 4 are not very smooth. This may be attributed to the fact that in some simulations the bubble diameter is still slightly changing, as discussed above.

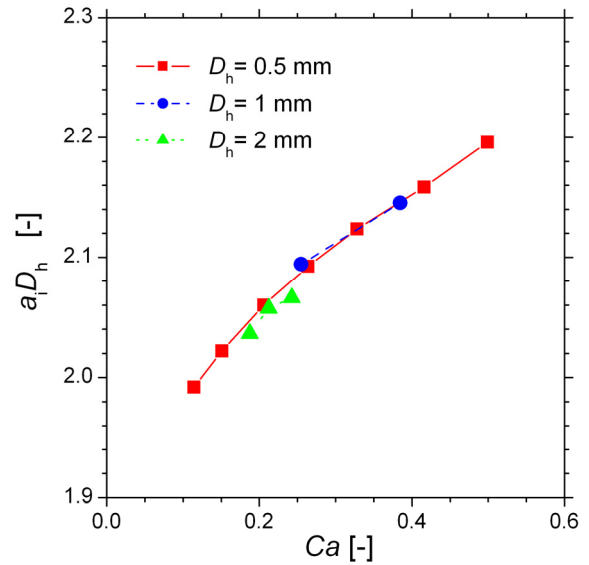


**Fig. 5** Non-dimensional volumetric interfacial area in the unit cell as function of the capillary number.

### 3.4 Volumetric interfacial area

For mass transfer applications the interfacial area per unit volume  $a_i = A_B / V_{uc}$  is of great importance. Here,  $A_B$  is the surface area of the bubble and  $V_{uc} = L_{uc} D_h^2$  is the volume of the unit cell. In Fig. 5 we show the non-dimensional volumetric interfacial area  $a_i D_h$  for the different cases as function of  $Ca$ . Again, the data for the different channels collapse to one single curve.

## 4. Conclusions

In this paper, we numerically studied the influence of the channel size on co-current downward Taylor flow in a square channel and performed simulations for three different hydraulic diameters ( $D_h = 0.5$  mm, 1 mm, 2 mm). In these simulations, the range of the capillary number, Reynolds number and Eötvös number is  $0.114 \leq Ca \leq 0.499$ ,  $1.56 \leq Re \leq 13.23$  and  $0.0667 \leq Eö \leq 1.068$ , respectively. The results for the three channels sizes show that the ratio  $U_B / J$ , the non-dimensional bubble diameter  $D_B / D_h$  and the non-dimensional volumetric interfacial area  $a_i D_h$  scale with the capillary number  $Ca$  while the influence of the Reynolds and Eötvös number (i.e. that of inertial and buoyancy forces) is very small and almost negligible for the range of parameters investigated.

Since in some of the present simulations the bubble length and diameter are still slightly changing in time, these runs are continued. Furthermore, additional simulations for  $D_h = 4$  mm and 8 mm are planned in order to cover the entire range of hydraulic diameters of monolith reactors.

## Acknowledgment

The author thanks A.N. Boran from Sakarya University (Turkey) who performed some of the numerical simulations during her Erasmus stipend at Karlsruhe Institute of Technology. He also acknowledges the support of Deutsche Forschungsgemeinschaft by grant WO 1682/1-1 within priority programme "Transport Processes at Fluidic Interfaces" (SPP 1506).

## Nomenclature

$A_B$	= surface area of the bubble (m <sup>2</sup> )
$a_i$	= volumetric interfacial area (1/m)
$C_0$	= distribution parameter (-)
$Ca$	= capillary number (-)
$D_B$	= maximum bubble diameter (m)
$D_h$	= hydraulic diameter (m)
$Eö$	= Eötvös number (-)
$Eu_{ref}$	= reference Euler number (-)
$Fr_{ref}$	= reference Froude number (-)
$g$	= gravitational acceleration (m/s <sup>2</sup> )
$J$	= superficial velocity (m/s)
$L_{ref}$	= reference length (m)
$L_{uc}$	= length of the unit cell (m)
$\Delta p_{uc}$	= pressure drop along unit cell (Pa)
$Re$	= Reynolds number (-)
$U_B$	= bubble velocity (m/s)
$U_{G-J}$	= drift velocity (m/s)
$U_{ref}$	= reference velocity (m/s)
$V_{uc}$	= volume of the unit cell (m <sup>3</sup> )

## Greek letters

$\varepsilon$	= gas holdup in the unit cell (-)
$\mu$	= dynamic viscosity (Pa s)
$\rho$	= density (kg/m <sup>3</sup> )
$\sigma$	= coefficient of surface tension (N/m)
$\Pi_y$	= source term in axial momentum eq. (-)

## Subscripts

B	= bubble
G	= gas phase
L	= liquid phase
ref	= reference value
uc	= unit cell

## Literature Cited

- Bauer T. Experimental and theoretical investigations of monolithic reactors for three-phase catalytic reactions. PhD thesis, Technical University Dresden, 2007.
- Boger, T., Heibel, A.K., Sorensen, C.M. Monolithic catalysts for the chemical industry. *Ind. Eng. Chem. Res.*, **43**, 4602-4611 (2004).
- Bretherton, F.P., The motion of long bubbles in tubes. *J. Fluid Mech.*, **10**, 166-188 (1961).
- Guettel, R., Knochen, J., Kunz, U., Kassing, M., Turek, T. Preparation and catalytic evaluation of cobalt based monolithic and powder catalysts for Fischer-Tropsch synthesis. *Ind. Eng. Chem. Res.*, **47**, 6589-6597 (2008).
- Keskin, Ö., Wörner, M., Soyhan, H.S., Bauer, T., Deutschmann, O., Lange, R. Viscous co-current downward Taylor flow in a square mini-channel. *AIChE Journal*, **56**, 1693-1702 (2010).
- Kreutzer, M.T., Kapteijn, F., Moulijn, J.A., Heiszwolf, J.J. Multiphase monolith reactors: chemical reaction engineering of segmented flow in microchannels. *Chem. Eng. Sci.*, **60**, 5895-5916 (2005).
- Liu, H., Vandu, C.O., Krishna, R. Hydrodynamics of Taylor flow in vertical capillaries: flow regimes, bubble rise velocity, liquid slug length, and pressure drop. *Ind. Eng. Chem. Res.*, **44**, 4884-4897 (2005).
- Liu, W., Hu, J., Wang, Y. Fischer-Tropsch synthesis on ceramic monolith-structured catalysts. *Catalysis Today*, **140**, 142-148 (2009).
- Öztaskin, M.C., Wörner, M., Soyhan, H.S. Numerical investigation of the stability of bubble train flow in a square minichannel. *Phys. Fluids*, **21** 042108 (2009).
- Taylor, G.I., Deposition of a viscous fluid on the wall of a tube. *J. Fluid Mech.*, **10**, 161-165 (1961).
- Thulasidas, T.C., Abraham, M.A., Cerro, R.L. Bubble-train flow in capillaries of circular and square cross section. *Chem. Eng. Sci.*, **50**, 183-199 (1995).
- Wörner, M. Numerical evidence for a novel non-axisymmetric bubble shape regime in square channel Taylor flow. 7<sup>th</sup> Int. Conf. Multiphase Flow, Tampa, FL, USA, May 30-June 4, 2010.
- Zuber, N, Findlay, J.A. Average volumetric concentration in two-phase flow systems. *J. Heat Transfer*, **78**, 453-468 (1965).